Colloids and Surfaces A: Physicochemical and Engineering Aspects 654 (2022) 130135

Contents lists available at ScienceDirect

Colloids and Surfaces A: Physicochemical and Engineering Aspects

journal homepage: www.elsevier.com/locate/colsurfa

Solid lipid nanoparticles and nanostructured lipid carriers of dual functionality at emulsion interfaces. Part I: Pickering stabilisation functionality

Georgia I. Sakellari [a,*], Ioanna Zafeiri [a], Hannah Batchelor [b], Fotis Spyropoulos [a]

[a] School of Chemical Engineering, University of Birmingham, Edgbaston, Birmingham B15 2TT, UK
[b] Strathclyde Institute of Pharmacy and Biomedical Sciences, University of Strathclyde, 161 Cathedral Street, Glasgow G4 0RE, UK

HIGHLIGHTS

- The lipid matrix composition affects the interfacial tension reduction ability.
- The affinity of the lipid matrix components influences the lipid particle hydrophilicity.
- Both SLNs and NLCs can provide Pickering emulsion stabilisation.
- The lack of unadsorbed surfactant in the continuous phase affects the emulsion droplet size.
- The particles maintained close association with the emulsion interface for up to 12 weeks.

GRAPHICAL ABSTRACT

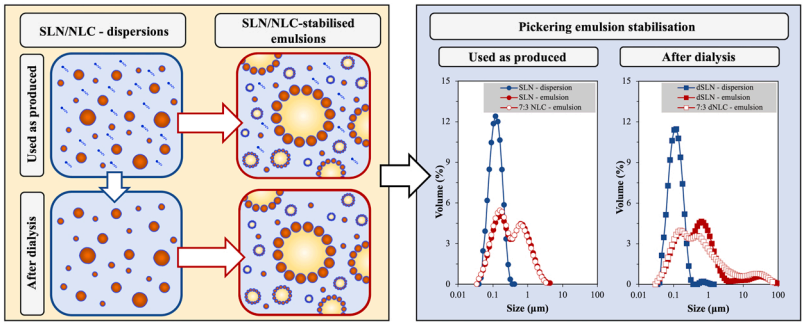

ARTICLE INFO

Keywords:
Solid lipid nanoparticles
Nanostructured lipid carriers
Interfacial characteristics
Wettability
Pickering functionality
Colloidal stability

ABSTRACT

Solid lipid nanoparticles and nanostructured lipid carriers are two types of lipid nanoparticulate systems, that have been primarily studied for their capability to function as active carriers, and only more recently utilised in Pickering emulsion stabilisation. Unveiling the factors that impact upon the lipid particle characteristics related to their Pickering functionality could enable the development of a liquid formulation with tailored microstructure and potentially the capacity to display a two-fold performance. In part I, this work investigates how certain formulation characteristics, namely solid-to-liquid lipid mass ratio and presence of unadsorbed surfactant in the aqueous carrier phase, affect the structural properties of the lipid particles, and in turn how these influence their Pickering stabilisation capacity. The effect of the formulation parameters was assessed in terms of the wettability and physicochemical properties of the lipid particles, including particle size, crystallinity and interfacial behaviour. Lipid particles fabricated with higher liquid lipid content (70% w/w) were shown to be more hydrophilic and have lower surfactant decoration at their surface compared to particles containing lower or no liquid lipid in their crystalline matrix. The emulsion stabilisation ability through a Pickering mechanism was confirmed for all types of lipid particles using polarised microscopy. Increasing liquid lipid content and removal of excess surfactant did not compromise the particle stabilisation capacity, though emulsion droplets of larger sizes were initially acquired in the latter case. The particle-stabilised emulsions maintained their physical integrity, with particles retaining close association with the emulsion interface over a storage period of 12 weeks.

* Corresponding author.
E-mail address: gis823@bham.ac.uk (G.I. Sakellari).

https://doi.org/10.1016/j.colsurfa.2022.130135
Received 14 July 2022; Received in revised form 3 September 2022; Accepted 6 September 2022
Available online 9 September 2022

1. Introduction

The development of formulations that can incorporate multiple actives with high loading capacities and deliver these in a controlled manner has more recently received significant research attention, with extensive applications in the food and pharmaceutical industries. Within this scope, emulsions stabilised by colloidal particles offer the versatility introduced by emulsions, not only due to the superior stabilisation capacity through a Pickering mechanism [1,2], but also for their potential to enable the segregated co-encapsulation of actives within discrete 'compartments' of their microstructure; i.e. the emulsion droplets and the Pickering particles themselves [3–5]. The aptitude of lipid nanoparticles, both solid lipid nanoparticles (SLNs) and nanostructured lipid carriers (NLCs), to function as active carriers has been widely discussed in literature and has been associated to numerous potential applications [6–9]. Besides their use as a delivery system, lipid particles (SLN in particular) have also been previously utilised in Pickering emulsion stabilisation [10–13]. However, the approach of 'expressing' these (Pickering stabilisation and active carrying) capabilities in tandem and within a single formulation, has only recently been explored [3,14]. Hence, the formulation characteristics and structural properties that influence this dual functionality, and how these both can be controlled/manipulated (without compromising one another), are still not clearly understood.

Thus far, due to the only recent emergence of literature in this area, there is a limited number of characteristics that have been identified for their crucial role in the design of lipid colloidal particles with potential to provide effective Pickering stabilisation. The solid lipid source and its crystalline state, dictated by the composition of the lipid matrix and the type of surfactant used, have been shown to entail great impact on the long-term stability of the SLNs within the emulsion systems with the occurrence of solid matter loss phenomena and weakening of their structural integrity, that could in turn impinge upon their Pickering functionality [11]. In the same study [11], where SLNs fabricated with either cetyl palmitate or tristearin were employed, it was shown that although the lipid source did not affect the initial droplet size, over time particle desorption from the interface of the emulsions stabilised with the latter was recorded. Schröder et al. [15] showed that lath-like particles, fabricated only with solid lipids, formed jammed interfacial layers and three-dimensional networks in the continuous phase of the emulsions, whereas thin interfacial layers were observed when particles comprising of solid and liquid lipids with platelet-like morphology were employed.

Other studies have discussed the importance of particle wettability [10,13,16,17], and more specifically how changes in the surfactant type and concentration can cause variations in the resulting interfacial layer morphology and SLN hydrophilicity/hydrophobicity [12,18]. Lim et al. [18] considered the effect of increased surfactant (particle) surface, not only on the enhanced hydrophilicity and reduced contact angle of the SLNs, but also on the improved emulsion stability that these can provide due to steric hindrances. It was therefore suggested that the interfacial and colloidal stability of SLN-stabilised emulsions could be enhanced by increasing the concentration of surfactant during SLN fabrication. The presence of excess surfactant in a continuous phase that also contains lipid particles can impact the affinity that the latter have for the emulsion interface. This has been shown for different particulate systems, such as hydrophobic hydroxypropyl methylcellulose (HPMCC) [19] or hydrophilic silica particles [20], and it was demonstrated that the use of surfactants with higher HLB value and concentration led to further interfacial tension reduction and improved stability. In lipid particle-stabilised emulsions, regardless of whether the SLNs are added in a pre-formulated emulsion [21] or if the emulsion is fabricated with the continuous phase comprising of the lipid particles prior or post-removal of excess unadsorbed surfactant [18,22], a fraction of the surface active species used to form the SLNs has been proposed [22] to migrate to the droplets' interfaces, ultimately creating a mixed emulsifier system (stabilised by both colloidal solid structures and surface active molecules). Overall, modifying the above characteristics that have been studied primarily for SLNs and only scarcely for NLCs, could expand current understanding on how an interfacial layer formed by colloidal particles can be controlled.

The aim of part I of this study is to enhance the understanding regarding the formulation characteristics of lipid (both SLN and NLC) particles that affect their interfacial properties and consequently their functionality as Pickering emulsion stabilisers. Hence, part of the work presented here focuses on the investigation of the extent to which the removal of excess unbound surfactant from the aqueous phase carrying the lipid particles affects their physicochemical characteristics, that have been known to impact on their Pickering functionality. The effect of the lipid composition and remnant surfactant removal on the particle wettability were also assessed. Thereafter, SLNs and NLCs with varying solid-to-liquid lipid mass ratios used as produced and after removal of unbound surfactant, were studied for their ability to stabilise o/w emulsions. Lipid particle-stabilised emulsions were characterised for their size distribution, zeta potential and long-term storage stability. Consequently, the insight gained from the findings of this study could contribute to extending the approaches that can be devised to intervene at a lipid particle level and manipulate the properties that enable the successful realisation of a Pickering functionality. As a lot of these characteristics have also been shown to impact on the capacity of lipid particles to carry and deliver actives, this work would also pave the way to successfully realise the dual functionality envisaged.

2. Materials and methods

2.1. Materials

Glyceryl behenate (Compritol® 888 ATO) was kindly provided from Gattefossé (Saint-Priest, France). Medium chain triglycerides (MCTs) (Miglyol® 812) was a kind gift from IOI Oleo (IOI Oleochemicals GmbH, Germany). Polyoxyethylene sorbitan monooleate (Tween® 80), perylene and Nile Red were purchased from Sigma-Aldrich (Sigma-Aldrich, UK). Sunflower oil was purchased from a local supermarket and stored in a closed container at ambient temperature in the dark. The consistency of the oil used in this work was monitored through interfacial tension measurements between distilled water and the used commercial oil (at least on a weekly basis). No significant deviation in the equilibrium value of the interfacial tension was observed (21.8 $\pm$ 0.3 mN/m). All chemicals were used without further purification. Double distilled water from Milli-Q systems (Millipore, Watford, UK) was used during all sample preparation processes and characterisation measurements.

2.2. Preparation of lipid particles

The lipid nanoparticle dispersions were fabricated following a protocol that is fully described elsewhere [6]. Briefly, solid and different solid-to-liquid lipid mass ratio (9:1, 8:2 and 7:3) lipid melts were processed with a melt-emulsification-ultrasonication method followed by quench cooling to obtain the crystalline lipid particles. All systems were composed of 2.5% w/w total lipid phase, and 1.2% w/w surfactant concentration in distilled water. Removal of excess unbound surfactant from the lipid dispersions was achieved through dialysis. A known amount of each dispersion was added in a cellulose dialysis membrane (43 mm width, 14 kDa M.W. cut-off, Sigma-Aldrich Company Ltd., Dorset, UK,), that was pre-hydrated overnight, and immersed in distilled water under constant stirring at room temperature. The dialysis medium was changed every 24 h and the process was continued until an equilibrium surface tension value similar to that of distilled water was obtained (~ 21 days). Surface tension measurements were performed with a profile analysis tensiometer (Pat-1M, Sinterface Technologies, Berlin, Germany). Further information about the instrument setup is given in a later section (*Section 2.5*). Following that, the lipid dispersions were

retrieved from the tubing and diluted to their initial mass with distilled water, to maintain the initial lipid phase concentration. All samples were stored at 4 °C until further analysis.

2.3. Particle size and ζ-potential measurements

Dynamic light scattering (DLS) was employed to determine the lipid particle size characteristics of dialysed and undialysed dispersions, and zeta potential (ζ-potential) of both lipid particles and their respective o/w emulsion systems using a Zetasizer Nano ZS (Malvern Instruments, UK). *Z*-average, polydispersity index (PDI) and ζ-potential values were acquired to assess the stability of the lipid particles dispersions after dialysis. All measurements were performed at a backscattering angle of 173° at 25 °C, and samples were appropriately diluted with distilled water to avoid multiple scattering phenomena. The refractive indices (RI) for the materials used were determined by a refractometer (J357 series, Rudolph Research Analytical, USA) at 20 °C, and used accordingly [6]. For distilled water, the refractive index used was 1.33 and the absorption index was set at 0.01. Measurements were performed immediately after preparation and over time in triplicate, and the average values with standard deviation (± S.D.) are presented. Representative size distributions of lipid particles used as produced and after dialysis were also acquired with laser diffraction (LD) using a Mastersizer 2000 (Malvern Instruments, UK) for comparison purposes. A more detailed description of the technique is provided below (*Section 2.8*).

2.4. Thermal analysis

The thermal behaviour of the lipid particle dispersions used as produced and after dialysis was determined by Differential Scanning Calorimetry (DSC) using a Setaram μDSC3 evo microcalorimeter (Setaram Instrumentation, France). The temperature was cycled between 20 and 80 °C at a heating rate of 1.2 °C/min. Information about peak temperatures and melting enthalpies was obtained using the Calisto Processing software. All enthalpy values and thermograms reported, are normalised for the amount of crystallising material present in the samples. All measurements were performed in at least triplicate on three individually prepared samples.

2.5. Surface and interfacial tension measurements

Interfacial properties at the oil/water interface were obtained with the pendant drop method utilising a profile analysis tensiometer (PAT-1M, Sinterface Technologies, Berlin, German), at 20 °C. A drop of the lipid particle dispersions (prior and after dialysis) was suspended via a straight stainless-steel capillary (3 mm outer diameter) in the sunflower oil phase contained in a quartz cuvette, with the cross-sectioned surface area remaining constant at 27 mm^2. When surface tension measurements were performed, the quartz cuvette was used empty. Data were collected until equilibrium was reached (standard deviation of the last twenty measurements was smaller than 0.05 mN/m). Density values of the samples were determined using a densitometer (Densito, Mettler Toledo, US), at 20 °C. All measurements were conducted in at least triplicate on three individually prepared samples.

2.6. Contact angle measurements

The effect of the lipid composition on wettability was assessed by melting (approximately at 80 °C) glyceryl behenate singly or in blends with medium chain triglycerides at different solid-to-liquid lipid mass ratios (9:1, 8:2, 7:3) and let to cool down at room temperature on a hydrophobic surface provided by a polydimethylosiloxane (PDMS) film to obtain a smoothly solidified lipid layer. The crystallised lipid was used to determine the contact angle (θ) of an oil droplet on the lipid surface following a previously proposed method with slight modifications [10]. Briefly, flat discs of solidified lipid or lipid blends were placed on top of a water-containing quartz cuvette, and a small volume (~ 10 μl) of sunflower oil was injected through a very small slit created during the crystallisation of the lipids using a micropipette, to create a pendant oil droplet. Images were acquired once equilibrium was reached, using a profile analysis tensiometer (PAT-1 M, Sinterface Technologies, Berlin, German) and the contact angles were determined with the angle-measuring tool of ImageJ. Similarly, to investigate the effect of the presence of excess surfactant on the hydrophilicity of the lipid particles, lipid particle dispersions used as produced and after dialysis were freeze dried and the powders obtained were compressed to obtain flat pellets of ~2 mm thickness using a universal material testing machine (Z030, Zwick Roell, Germany). A sessile drop (~ 10 μl) of distilled water was deposited on the surface of the pellet and the contact angle was measured according to the method described above. All measurements were performed in at least triplicate, the contact angle on both the left and right side were measured and the average θ values were calculated.

The free energy of displacement (ΔG_d) for a particle at the oil-water interface was calculated using the following equation [10]:

$$\Delta G_d = \pi r^2 \gamma_{ow} (1 - |cos\theta|)^2 \quad (1)$$

where *r* is the particle radius calculated from the *Z*-average values, and θ is the contact angle as determined above. The sunflower oil/water interfacial tension γ_{ow} was determined using the method described in the previous section (15.2 mN/m). In addition, the solid lipid-water γ_{sw} and solid lipid-oil γ_{sw} interfacial tensions were calculated as follows [10, 23]:

$$\cos\theta = \frac{(0.015\gamma_{ow} - 2)(\gamma_{ow}\gamma_{sw})^{1/2} + \gamma_{ow}}{\gamma_{ow}[0.015(\gamma_{ow}\gamma_{sw})^{1/2} - 1]} \quad (2)$$

$$\gamma_{ow}\cos\theta = \gamma_{sw} - \gamma_{so} \quad (3)$$

2.7. Preparation of oil-in-water emulsions

Oil-in-water (o/w) emulsions were prepared with 90% (w/w) aqueous phase containing any of the different lipid nanoparticle systems and 10% (w/w) sunflower oil phase. Emulsification was realised using a high intensity ultrasonic Vibra-cell™ VC 505 processor (Sonics & Materials, Inc., CT, USA), operating continuously at 750 Watt and 20 kHz, at a sonication amplitude of 95% of the total power over a period of 30 s. When different emulsification methods were assessed for their effect on the obtained droplet size, the parameters are summarised in Fig. 6. Samples were immersed in an ice bath during processing, to avoid shear-induced heating. The produced systems were stored at 4 °C until further analysis.

2.8. Droplet size measurements

The droplet size of the o/w emulsion droplets and their stability over time was assessed by laser diffraction (LD) using a Mastersizer 2000 (Malvern Instruments, UK) equipped with a Hydro SM manual small volume sample dispersion unit. Measurement parameters including RI values and absorption index were kept the same as for the particle size measurements described above. The stirrer speed was set at 1300 rpm during all measurements, and all samples were mixed by hand before analysis. The refractive index (RI) of sunflower oil was set at 1.47. Samples were analysed immediately after production and after 1, 4, 8 and 12 weeks. All measurements were performed in triplicate on three individually prepared samples.

2.9. Imaging

The microstructure of the prepared o/w emulsions was visualised through polarised light microscopy and confocal laser scanning microscopy (CLSM), to confirm the Pickering performance of the lipid

particles. The confocal microscopy images were obtained using a confocal laser light microscope (Leica TCS SPE, Heidelberg, Germany), equipped with a laser operating at a wavelength of 532 nm. For the visualisation of the different components of the emulsion systems, dyes with different excitation wavelengths were employed. Perylene (0.005% w/w) was used to stain the lipid particle dispersions, by addition to the lipid melt phase prior to ultrasonication, and Nile Red (0.005% w/w) was added to the sunflower oil phase, prior to emulsification. The excitation wavelength for Nile Red was set at 488 nm and 405 nm for perylene. The polarised light microscopy images were acquired with an optical microscope (DM 2500 LED, Leica®, CH). When larger emulsion droplets were visualised using both analyses, the emulsions were prepared using a low level of shear provided by a high-shear mixer (Silverson L5 M, Silverson Machines Ltd, UK), operating at 9000 rpm for 2 min, and the images were acquired with a 100x oil immersion lens using a coverslip to cover the sample.

2.10. Statistical analysis

Samples were analysed in at least triplicate and averages are reported with standard deviation. Figures depict the calculated average value with error bars showing the standard deviation above and below the average. Comparison of means was conducted by ANOVA analysis followed by an all pairwise multiple comparison test using the Student-Newman-Keuls Method (SigmaPlot 14.5). The differences were considered statistically significant when $p < 0.05$.

3. Results and discussion

3.1. The effect of excess surfactant on the physicochemical characteristics of lipid particles

Among the parameters that can affect the physicochemical properties of the lipid particles while in an aqueous dispersion environment, and subsequently their effectiveness to act as Pickering emulsion stabilisers, is the presence of excess unadsorbed surfactant in their continuous phase. A sufficient excess concentration of surfactant in the aqueous phase carrying the lipid particles is required during their fabrication, to ensure rapid adsorption of the surfactant molecules on the particle surfaces, which is a crucial parameter in preventing particle-particle collisions and particle destabilisation phenomena [24]. Therefore, previously studied and characterised SLNs and NLCs of different solid-to-liquid lipid mass ratios (9:1, 8:2 and 7:3) were dialysed to remove any excess surface active species. The process of the unadsorbed

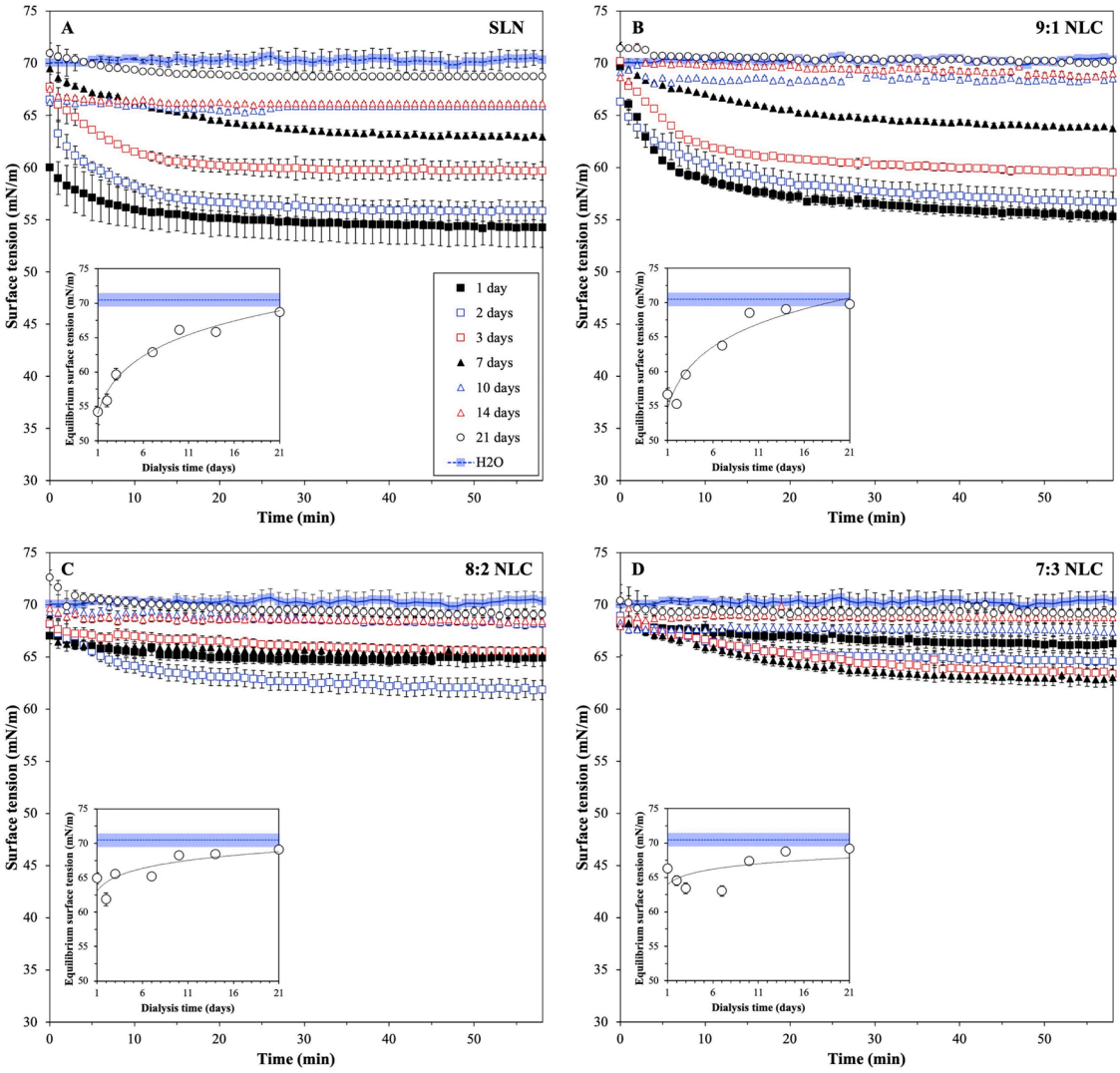

Fig. 1. Surface tension of aqueous lipid particle dispersions of SLN (A), 9:1 NLC (B), 8:2 NLC (C) and 7:3 NLC (D) at various time points during dialysis. The inset graphs for each type of lipid particle dispersion depict the time evolution of the equilibrium surface tension values over the dialysis period. The surface tension of distilled water is also presented as a comparison. When not visible, error bars are smaller than symbols.

surfactant removal was monitored with surface tension measurements of the dissolution medium (Fig. 1), and the effect that this had on the size, ζ-potential, thermal behaviour and interfacial tension reduction ability of the particles was investigated (Figs. 2–4).

The amount of surface active species associated with the surface of the lipid particles is an important parameter that can dictate not only their functionalities, but also their long-term physical stability. In this study, investigation of the surface load (Γ_s) can provide information regarding the relative association of the surfactant with the lipid matrix composition, as well as the effect that this has on the interfacial properties of the aqueous lipid particles. As presented in Fig. 1*A-D*, there is progressive flattening of the surface tension curvature for all formulations, with the curves being similar to that of distilled water at 21 days. More specifically, the rate of surfactant loss appeared to be similar for the SLN and 9:1 NLC formulations, and also for the 8:2 and 7:3 NLC systems (*inset graphs,* Fig. 1). The first pair shows an initial fast diffusion rate that only decelerates at day 10, whereas the removal of surfactant for the latter group (8:2 and 7:3 NLCs) seems to occur in a steadier rate. Although based on the available data it is not possible to determine the degree of contribution of each possible mechanism to the observed difference, two factors could be pointed out, according to variations identified in the used systems. The first stems from disparities in the total surface area available, with smaller particle sizes (Fig. 2) in the latter pair (particles with the highest liquid lipid content), allowing for a larger surface area to entrap the available surfactant, and hence a lower concentration of Tween® 80 discharging to the acceptor phase. The second could be attributed to differences in the lipid mixtures composition affecting the dynamics of surfactant exchange between the particle surface and the continuous phase, that further impacts the diffusion rate.

In order to compare with literature data, the surface load was calculated using the equation described by Dickinson [25] (Equation S1). This was done by presuming that the particles are spherical in shape, and following the assumption that the entirety of the available surfactant molecules ($C_{a,max}$) is adsorbed and/or associated with the surface of the particles, based on which the calculated values would correspond to the maximum achievable Γ_s (Supplementary Information). In a study investigating the impact of sonication during crystallisation and liquid lipid content, Ban et al. [26] reported that the surface load varied from 6.34 mg/m^2 for the SLN, to 7.50 mg/m^2 belonging to the 7:3 NLC formulation, while there was a proportional relationship between liquid lipid content and surface load. In another work by the same authors [27], increased Γ_s was observed with increasing surfactant concentration until saturation was reached at lower values for surfactants with saturated chains (34 mM) compared to unsaturated (65 mM) on the tristearin (5 % w/w) SLN surface. Analogous results of Γ_s increase with increasing surfactant concentration were obtained for tristearin particles (2.5 % w/w lipid phase), with values starting at 9 mg/m^2 for 10 mmol/kg concentration of Tween® 60 and Brij® S20, reaching 15 and 19 mg/m^2 for 24 mmol/kg, respectively, and 25 mg/m^2 for 8 mmol/kg Brij® S100 concentration [18]. The Γ_s values calculated here were 9.6 mg/m^2 for the SLN and 9:1 NLC formulations, 8.4 mg/m^2 for the 8:2 NLC and 8.7 mg/m^2 for the 7:3 NLC systems. These values, that correspond to 1.2 % w/w (or 10.1 mmol/kg) concentration of Tween® 80 % and 2.5 % w/w lipid phase, are within the value range reported in literature for similar particle size and lipid phase-to-surfactant mass ratio [24,28]. The fact that they are slightly closer to the higher end of the value spectrum could be attributed to the longer unsaturated hydrophobic tail of Tween® 80, and also the different lipid/surfactant combination used in this study, allowing for greater participation of surfactant molecules in the crystalline lattice of the lipid particles, thus resulting in higher Γ_s [6,27]. Additionally, the presence of lipid particles that are non-spherical, as suggested by the presence of different polymorphs in the DSC thermograms of the lipid dispersions, could explain the requirement for a higher surfactant concentration to saturate the lipid particle surfaces compared to only spherical structures [24,28–30]. Variations in the surfactant molecule orientation and packing at the particle surface could be the cause of the surface load deviations between the different types of lipid particles [18]. However, it should be highlighted here, that for the Γ_s calculations, several assumptions were made, including sphericity of the particles and considering that the entirety of the available surfactant was associated with the particles. This is not necessarily a realistic representation of the particle state, but rather an attempt to set the scene for the surface coverage of the examined particles using a marginal scenario, as a small but detectable proportion of the initially added surfactant was removed, according to the surface tension measurements. Therefore, to improve the theoretical picture drawn for the quantity of surfactant associated with the particles, the minimum concentration of Tween® 80 ($C_{a,min}$) required to form a monolayer at the interface of the particles was also calculated (Supplementary Information). According to the theoretical calculations, the minimum concentration required to fully cover the particle surface would be 0.5 % w/w for the SLN and 9:1 NLC formulations, and 0.6 % w/w for the 8:2 and 7:3 NLCs, suggesting that there was an excess of approximately 50 % of Tween® 80 concentration used to prepare the particle dispersions (1.2 % w/w used during fabrication). Based on both

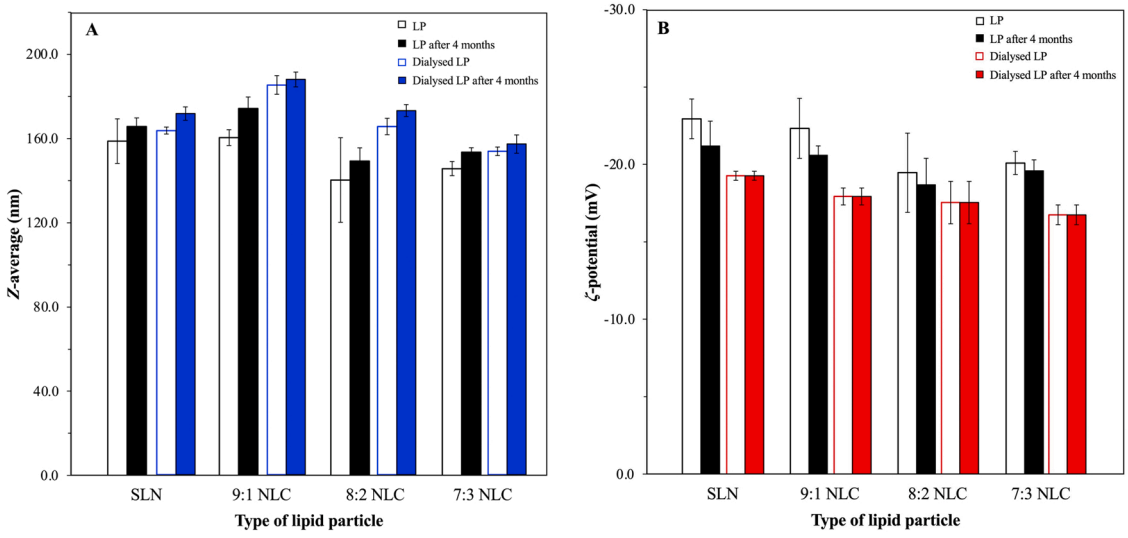

Fig. 2. Particle size (Z-average) (A) and zeta potential (ζ-potential) (B) of lipid particle dispersions (LP) before and after dialysis measured immediately after production and after 4 months of storage.

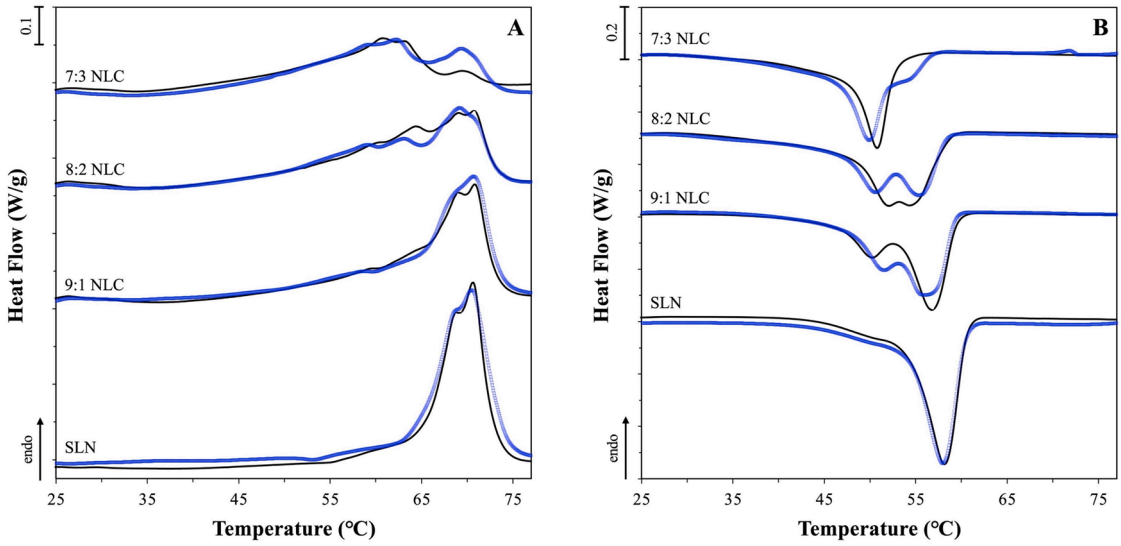

Fig. 3. Melting (A) and crystallisation (B) curves of SLN and NLC aqueous dispersions before dialysis (black curve) and after 4 months of storage following removal of excess surfactant (blue curve).

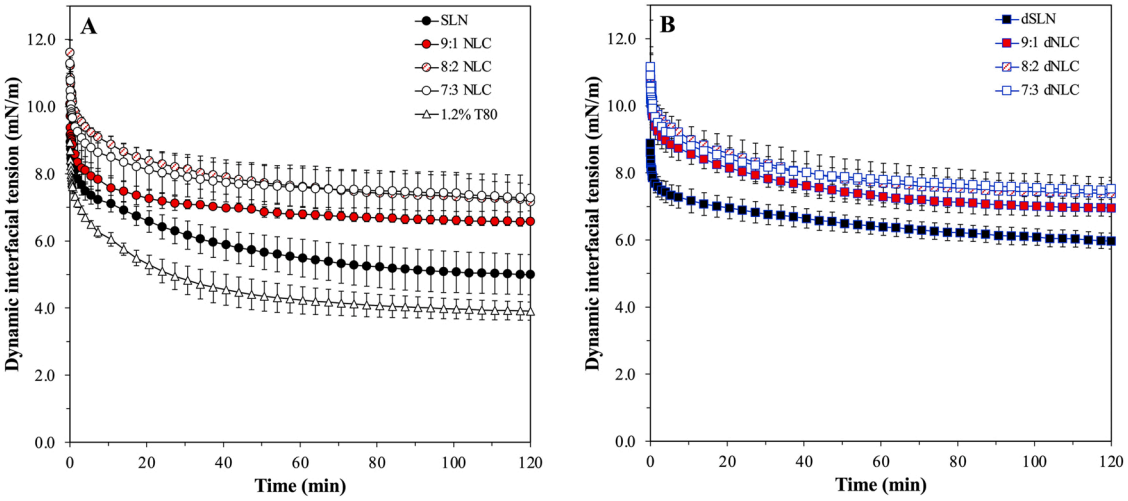

Fig. 4. Dynamic interfacial tension of aqueous dispersions of SLN and NLC formulations before (A) and after dialysis (B). The curve of pure Tween® 80 (T80) solution with similar concentration (1.2% w/w) as the one used for the formulation of the dispersions is also presented for comparison. Data points are the average of three measurements and error bars represent the standard deviation.

the assumptions for the maximum surface load and the theoretical calculations for the minimum concentration of adsorbed surfactant, it could be hypothesised that the true value of surfactant concentration associated with the particles lies between these two predictions. Due to the hypotheses adopted and the overall theoretical nature of these calculations, the results presented above should only be perceived as a qualitative characterisation, rather than an attempt to quantitively describe the systems.

3.1.1. *Particle size and zeta potential*

Regarding the effect of excess surfactant removal on the size of the lipid particles, it is evident from Fig. 2A, that the *Z*-average slightly increased immediately after dialysis for all types of NLCs, while the increase was not statistically significant for the SLNs. Changes in the steric hindrance-induced stability due to the removal of free surfactant molecules, and the osmotic stress applied to the dispersions during the diffusion of the molecules through the dialysis membrane could have promoted flocculation and aggregation, as further supported by increase in the PDI values (Fig. S1). On the other hand, the ζ-potential decreased for all formulations (Fig. 2B), with the exception of 8:2 NLC. This could be due to small but considerable for their effect on the ζ-potential, variations in the viscosity of the formulations after removal of excess surfactant, and more prominently, aggregation of the particles after dialysis, as Tween® 80 is a non-ionic surfactant, and thus does not contribute to the charge of the electric double layer. Both the possibility of decrease in the dynamic viscosity values from 1.1 to 1 mPa·s (according to literature data for similar concentrations of surfactant) [31], causing changes in the mobility of the particles [32,33], and the presence of particle aggregation [34,35] could have ultimately resulted in the observed statistically significant decrease of the absolute ζ-potential values. Small but statistically significant differences in both the *Z*-average and ζ-potential values recorded between the different types of particles could have been caused by discrepancies in the arrangement of the hydrophilic heads of the surfactant at the surface of the particles and/or the depth of association with the surface [18,27,36]. The surface of the lipid particles is not fully covered by the surfactant molecules [6], and this is further supported by the negative ζ-potential arising from the free fatty acids at the surface of the particles [37].

3.1.2. Crystallinity

The crystallinity of the lipid particles was assessed after dialysis to determine changes in the properties of the crystalline matter after surfactant removal (Fig. 3). Previous work regarding the SLN and NLC formulations revealed that increase in the liquid lipid concentration leads to increasing loss of lipid phase crystallinity and more pronounced polymorphic transitions, as suggested by the melting enthalpy (ΔH), recrystallisation indices (RI) and both the melting and crystallisation thermograms (Fig. 3A & B) [6]. Comparing the thermograms of the lipid particle dispersions after preparation and after 4 months of storage following dialysis, no major differences can be identified in their melting and crystallisation profiles. Their ability to maintain their crystallinity is further confirmed by their melting enthalpies for which no statistically significant deviations were recorded (Fig. S2). Overall, it appears that removal of excess surfactant from their aqueous phase did not affect their crystalline structure.

3.1.3. Interfacial tension

As part of gaining further insight regarding the capability of the SLN and NLC formulations to exhibit a Pickering functionality, the sunflower oil/water dynamic interfacial tension was assessed using the different lipid particle dispersions as the aqueous phase. In addition, the presence of unadsorbed surfactant in the aqueous continuous phase of the lipid particle dispersions, and its effect on the dynamic interfacial tension reduction was further investigated by comparing the behaviour of the lipid particle systems before and after dialysis (Fig. 4).

For particles used as prepared, the interfacial tension reduction ability appears to be lower than that of equal concentration of surface active species in aqueous phase (1.2 % w/w) (Fig. 4A). Similar data have been previously reported for solid lipid nanoparticles with varying particle sizes, fabricated with different types of lipid materials and with surface active species having a range of distinct characteristics (i.e. molecular weight and/or HLB value) [17,22,38]. The comparison between lipid particles with different solid-to-liquid lipid mass ratio reveals that as the liquid lipid increases, the ability of the system to lower the interfacial tension decreases, with particles containing 20 % and 30 % w/w liquid lipid having almost identical dynamic interfacial tension curves. More specifically, the SLN formulation reached an equilibrium value of 5 mN/m, 6.6 mN/m was the value for the 9:1 NLC, and 7.2 and 7.3 mN/m were the equilibrium interfacial tension values for the 8:2 and 7:3 NLCs, respectively. The efficiency of the surfactant to alter the interfacial curvature is highly influenced both by the distribution of the surfactant molecules in the dispersion, and also by their packing characteristics [19]. The latter is not only relevant to the molecular packing density at the oil/water interface, but it also relates to potential lipid crystalline network participation [17,38]. In this instance, the interfacial affinity of the lipid particles for the oil/water interface, possibly conferred by their surfactant-decorated surfaces, could be influenced by the level of surfactant decoration. Considering that the only variation between the aqueous lipid particle dispersions is the composition of the lipid matrix, it could be proposed that the higher interfacial tension values for the systems containing higher liquid lipid percentages (9:1, 8:2 and 7:3 NLCs) is the result of the preferential trapping of surfactant molecules in the solid crystal/liquid oil crystal network interfaces. This is in accordance with what was previously hypothesised for the formulations presented here, regarding the relatively high compatibility between the lipid core components, particularly in the presence of increased MCT content and Tween® 80, and the involvement of the latter in the crystalline network, based on DSC data [6]. In terms of the effect of particle size, the results reported are somewhat contradictive to what would be expected for the larger particle sizes of the SLN and 9:1 NLC formulations. However, the seemingly unsubstantial impact of particle size on the interfacial tension reduction ability of the particles could be due to the much greater effect of the previously discussed parameters.

A more comprehensive understanding of the mechanism via which these systems lower the interfacial tension of the sunflower oil/water interface can be gained through investigation of the behaviour of the dispersions after removal of excess surfactant from the continuous phase. Comparing the obtained curves and equilibrium values, it was observed that only the SLN formulation (dSLN) presents a small but statistically significant increase in interfacial tension after dialysis (Fig. 4B). Taking into consideration that only marginal changes were recorded in the particle characteristics after processing, it could be postulated that this is the effect of presence of free surfactant molecules in the continuous phase of the SLN dispersion, possibly due to the high internal crystalline arrangement of the SLN lipid core. On the contrary, the lack of variation in the behaviour of the dialysed NLC formulations compared to the undialysed (9:1 dNLC, 8:2 dNLC and 7:3 dNLC) most likely suggests that the vast majority of surface active species present in the samples are associated with the surface of the lipid particles, and therefore not available to interact with the oil/water interface. Exchange of surfactant molecules between the lipid particles and the o/w interface has been proposed as a possible phenomenon in such dynamic systems, though it would entail that the surfactant molecules are easily displaced from the particle surface, due to their unfavourable trapping in the lipid core [21,22,39]. There is very limited literature discussing the interfacial tension alteration mechanism in the presence of lipid particles. Zaferi et al.[38] and Li et al.[17] showed that in the presence of SLNs, the interfacial tension reduction potential of the surfactant is lower than that of the pure surface active species solution in the absence of SLNs. Dieng et al.[22] suggested that once the SLNs arrive at the oil/water interface, part of the adsorbed surfactant (in which case was Kolliphor® HS15) is released, resulting in a conjugated particle/surfactant molecules adsorption mechanism. Linking the contradictory observations made here, regarding the greater interfacial tension reduction ability of the SLNs and the higher surface load values reported previously (*Section 3.1*), it is suggested that the level of decoration of the surfactant molecules on the surface of the particles is the interfacial tension reduction limiting factor, rather than the concentration of free molecules. Although no final conclusions can be drawn about the exact mechanism of participation of the lipid particles in the interfacial tension (e.g. occurrence of inter-particle or particle/free surfactant molecule interactions), it is clear that changes in the composition of the lipid particles and therefore in the adsorbed surfactant arrangement, and co-adsorption of particles and surfactant play an important role in the final interfacial curvature.

3.2. Wettability

Another parameter that was evaluated regarding the ability of the particles to stabilise emulsion droplets and their positioning at the sunflower oil/water interface was their wettability [40–42]. Following the method described by Gupta et al.[10], the effect of increasing liquid lipid content (0–30 % w/w) on the contact angle of a sunflower oil droplet at the lipid mixture/water interface was initially evaluated (Fig. 5A). The contact angle values ranged from 130.6° for the pure glyceryl behenate (SLN) surface to 147.6° for the 30 % w/w MCTs concentration (7:3 NLC). Homogeneous distribution of MCTs in the mixtures with glyceryl behenate led to progressively increased hydrophilicity of the blend, resulting in higher contact angles and thus lower wettability by the hydrophobic sunflower oil droplet. Using the experimental contact angle and γ_{ow} values and Eq. 2 & 3, the γ_{sw} and γ_{so} were calculated for each system. In every case, the condition $\gamma_{ow} > \gamma_{so} - \gamma_{sw}$ was satisfied, indicating efficient wetting by both phases, and positioning of the particles at the oil/water interface. Furthermore, the free energy of displacement ΔG_d was found to be an order of magnitude lower than that for similar systems reported in literature [10], ranging between $3.7 \times 10^4 \times k_B T$ for glyceryl behenate to $0.62 \times 10^4 \times k_B T$ for the 30 % w/w liquid lipid content blend. Though not vastly lower, the ΔG_d values show a decline with increasing MCTs content (Fig. 5A). Since ΔG_d depends on the square of the particle radius and the $\cos\theta$, it is

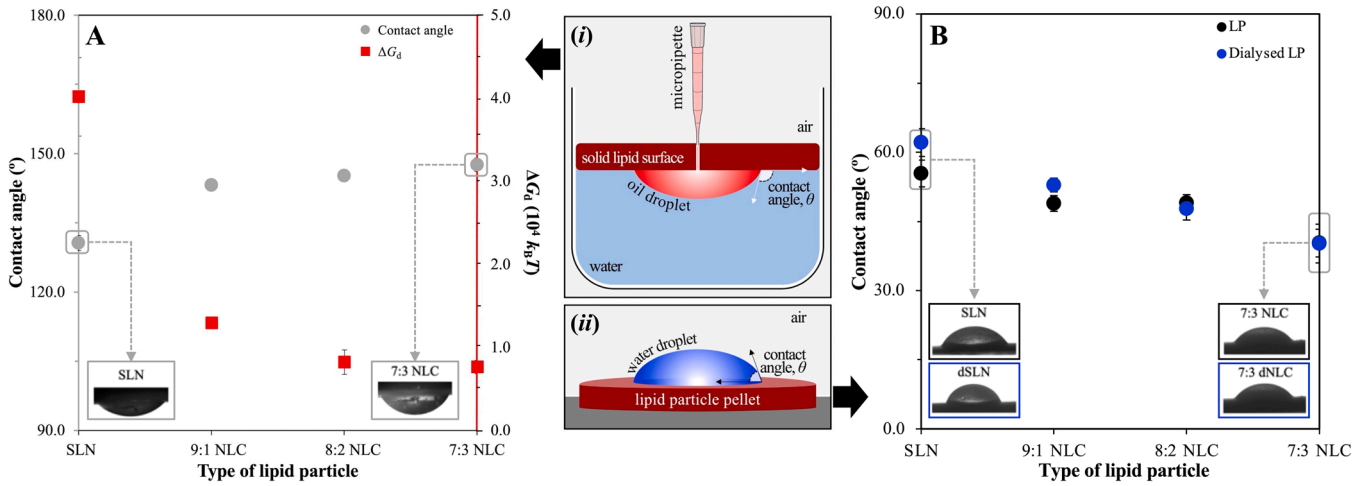

Fig. 5. Contact angle for a sunflower oil droplet at the water/solid interface, and displacement energy (ΔG_d) of the lipid particles at increasing liquid lipid concentration (0–30% w/w (A). The lipid content used to prepare the solid interfaces employed for the contact angle measurements represent the lipid matrix composition of the respective lipid particles. Contact angle for a water droplet at the air/particle interface formed by freeze dried powder of lipid particles used as produced and after dialysis (B). The experimental setup is also provided in a schematic representation. When not visible, error bars are smaller than symbols.

expected to have lower values for smaller particle radii and larger contact angles, which explains the trend observed for increasing liquid lipid content.

Besides the nature of the lipid used itself, the level of surfactant decoration on the particle and any excess surfactant within the aqueous carrier system could also contribute to the affinity between a lipid particle and an interface. It has been shown that incorporation of surfactant within the lipid particles in the first place can lower the water/lipid particle contact angle by reducing the hydrophobicity of the bulk lipid [43]. Delving further into the effect of the degree of surfactant decoration on a lipid particle, it has been proposed that surface load can be used as a means of controlling the obtained ΔG_d and particle wettability, by altering their hydrophilicity [18]. Therefore, it would be expected that as the proportion of surfactant associated with the particles increases with increasing liquid lipid content, based on previous indications provided by interfacial tension measurements, so would their hydrophilicity. Indeed, this was confirmed by the decreasing contact angle values obtained for increasing MCTs content (Fig. 5*B*). Notably, the difference in the hydrophilicity of the surface was statistically significant only for the SLN and 9:1 NLC formulations, when freeze dried powders were used after removal of excess surfactant, further reinforcing the evidence provided above regarding the influence of the lipid composition on the favourable surfactant entrapment. Overall, based on the contact angle data and the high energy of desorption obtained for all systems, it could be postulated that the particles fabricated with these lipid combinations will be preferentially wetted by the aqueous phase and therefore will be able to effectively stabilise o/w emulsion droplets [40,44].

3.3. Production and characterisation of particle stabilised emulsions

3.3.1. Processing of emulsions

The ability of lipid particles to stabilise o/w emulsions through a Pickering mechanism was investigated using SLNs as the continuous phase and sunflower oil as the dispersed phase. During preliminary studies, emulsions in the presence of SLNs were prepared employing a range of processing conditions of varying energy input. Fig. 6A depicts the average droplet size ($D_{4,3}$) of all emulsions produced, with the processing parameters employed also given. Sonication led to smaller droplet sizes (<1 μm) compared to methods that provide a lower level of shear, such as high-shear homogenisation. In addition, emulsions prepared with high-shear homogenisation, exhibited an oil layer formation and increased droplet sizes over storage, that indicate the occurrence of coalescence. Among the various sonication parameters that were examined, pulsed processes are known to alleviate the risk of heat-induced destabilisation phenomena, in this instance relevant to the lipid particles. However, it was shown that sonication for 30 s (method 5) without the use of pulser produced the most physically stable systems (no oil layer formed) over an observation period of 30 days, possibly due to the continuous delivery of high level of energy. Thus, that was the processing method chosen in later steps.

In order to assess whether the SLNs present in the system contributed to the stability of the produced emulsions, the microstructure of the emulsions was visualised using light microscopy, polarised light microscopy and confocal laser scanning microscopy CLSM (Fig. 6B-D). o/w emulsions with SLN were prepared following method 5 to confirm the Pickering stabilisation when using the preferred processing route (Fig. 6B), but also with method 3 to better visualise the microstructure of the emulsions (Fig. 6C & D). Images were acquired within 1–2 h after their fabrication. The Maltese cross birefringence pattern at the emulsion droplet surface (Fig. 6C) provides confirmation of the close association between the crystalline lipid particles (possibly containing a lamellar phase [45]) and the emulsion surface [15]. Similarly, the presence of particles adsorbed at the droplet interface was further supported by CLSM micrographs of particles loaded with perylene and emulsion droplets containing Nile Red (Fig. 6D) [11]. It was also observed that non-spherical, elongated droplets were also present in the samples, that could be attributed to the strong adsorption of the lipid particles, creating a jammed interface, hence preventing droplet shape relaxation, that has been previously reported for lipid particle stabilised o/w emulsions [15,18,46].

3.3.2. Droplet size and zeta potential

Following the processing method described above, 10 % o/w emulsions were prepared using the dispersions as the aqueous continuous phase. Lipid particles with varying liquid lipid content used as produced and after dialysis were employed, at a constant concentration of 2.5 % w/w of the aqueous phase. The size distribution graphs of the emulsions prepared in the presence of lipid particles used as produced (Fig. 7A) showed a bimodal distribution, with a peak at ~0.150 μm which is suggested to correspond to excess lipid particles (non interfacially adsorbed), and a second population at ~1 μm belonging to the produced emulsion droplets. Emulsions prepared with dialysed particle dispersions (Fig. 7B), displayed an additional (but much smaller) peak at larger droplet sizes, that appeared consistently in all formulations. In fact, in either case, the size distribution of emulsions prepared with different

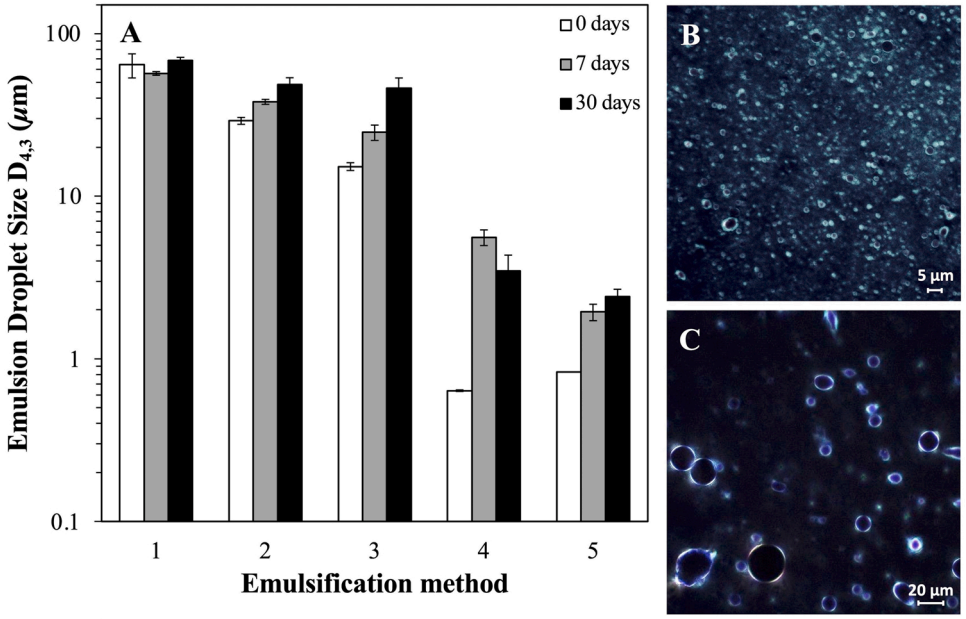

Method	Processing conditions
1	Ultra Turrax, 7000 rpm, 1 min
2	High-shear mixer, 7000 rpm, 1 min
3	High-shear mixer, 9000 rpm, 2 min
4	Sonication with pulser operating for 20 s on – 10 s off (40 s sonication), 95% amplitude
5	Sonication, 30 s, 95% amplitude

Fig. 6. Average droplet size of o/w emulsions with solid lipid nanoparticles prepared with different processing conditions at 0, 7 and 30 days (A). Representative images of SLN-stabilised o/w emulsions fabricated following methods 5 and 3 and acquired within 3 h after production using polarised light microscopy (B and C, respectively), and CLSM of system prepared with method 3 (D).

types of lipid particle dispersions showed an almost identical behaviour, with excess amount of unadsorbed lipid particles remaining in the continuous phase, possibly suggesting that the droplet formation is a process dominated by the process type rather than the properties of the lipid particles (e.g. hydrophilicity). The interfacial adsorption of particles in all cases was corroborated by optical microscopy (inset graphs,

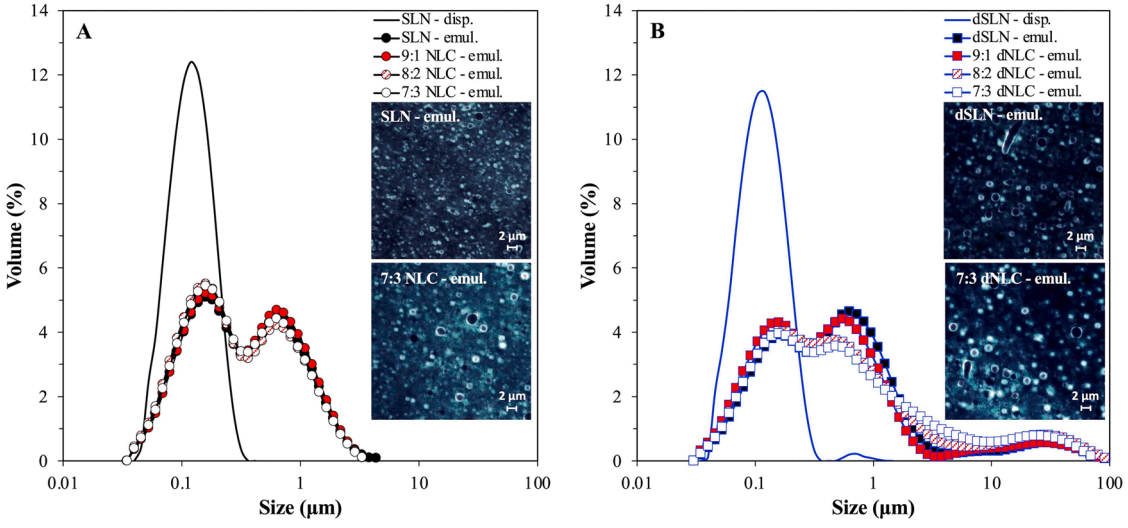

Fig. 7. Droplet size distribution of 10% o/w emulsions containing lipid particles with varying liquid lipid mass ratios (SLN, 9:1, 8:2 or 7:3 NLCs) used as produced (A) and after dialysis (B). The size distribution of the SLN formulation used as prepared and after removal of excess surfactant acquired using LD is also presented as a representative particle size example for comparison purposes in each graph, respectively. Representative polarised light microscopy images of SLN and 7:3 NLC-stabilised emulsions are provided in both graphs (inset graphs).

Fig. 7). The presence of larger emulsion droplets in the systems with dialysed lipid particles could be ascribed to various factors, among which is the limited availability of surfactant molecules during emulsification. In contrast to lipid particles, surfactant molecules can move promptly at the interface of the droplets and reduce the interfacial tension, subsequently preventing the droplet size increase [47,48]. This is particularly noticeable for the SLN formulation, as the interfacial tension measurement for the as produced dispersion suggested statistically significant higher levels of interfacial tension reduction compared to that used after dialysis (Fig. 4). This could have led to formation of smaller emulsion droplets in the former during emulsification. Although the interfacial tension between undialysed and dialysed NLCs did not show any statistically significant changes, the same droplet size trend as for the SLNs was observed. Another contributing factor could be the presence of excess surfactant in the continuous phase, that was previously demonstrated to increase the particle wettability by the aqueous phase based on contact angle data on one hand, and on the other hand increase the continuous phase viscosity (*Section 3.1.1*). Similar data were reported for MCT o/w emulsion droplets stabilised by cyclodextrins in the presence of Tween® 80, where increased surfactant concentration resulted in crystal movement towards the continuous phase, either due to replacement or faster adsorption of surfactant molecules to the interface [49]. Correspondingly, it could be suggested here, that the presence of excess surfactant in the aqueous phase of the lipid particle dispersions moved the particles away from the interface and closer to the water phase, which could in turn potentially provide improved steric hindrance against droplet collisions. What is more, even small differences in the viscosity of the continuous phase, due to the presence of additional surfactant, could have impacted the droplet size reduction aptitude [33,49]. Lastly, droplet aggregation, and additionally lower number of lipid particles for the same initial solid lipid phase concentration in the dialysed dispersions, due to the previously discussed particle size increase could have also contributed to the enlargement of the emulsion droplets [22].

In terms of the ζ-potential, when the lipid particles were used as produced, the resulting emulsions had a negative charge of ~− 29 mV, while for particles after dialysis the charge had a higher absolute value of ~− 34 mV (Fig. 8A). Consistently with the size distribution data, there were almost no differences in the ζ-potential values recorded among the different types of lipid particle dispersions. Comparing the surface charge of the particles alone to that of the respective particle-stabilised emulsions (in the range of −20 mV and −30 mV, respectively), it is observed that the emulsions displayed a higher charge that was statistically significant. More specifically, the difference between the lipid particle and the lipid particle-stabilised emulsion ζ-potential values was greater for the dialysed particles than that of the particles used as prepared, although the dialysed particles (alone) exhibited a lower surface charge (expressed as absolute values). In order to further explore why this was instigated, the theoretical number of lipid nanoparticles required to form a packed monolayer at the emulsion interface and the number of particles introduced during emulsification were calculated. These were correlated and expressed as percentage of particle excess (Fig. 8B). For this, the particle *Z*-average and the droplet $D_{3,2}$ values, as measured immediately after preparation (Table S1), were used to estimate the total number of lipid particles and emulsion droplets present in each system, assuming spherical shape in both cases, while the hexagonal packing correction was applied for the calculation of the maximum number of particles per emulsion droplet (Supplementary Information). As depicted in Fig. 8B, for particles with only slight variations in their average sizes when used as produced and after dialysis, the quantity required to fully cover the emulsion droplets decreases with increasing droplet diameter. However, in both instances there was an abundance of particles available in the continuous phase of the emulsions, the percentage of which was dictated mainly by the droplet surface. Based on the higher emulsion surface charge values obtained for the emulsions stabilised by dialysed lipid particles and the negative charge contribution of sunflower oil [50], it could be hypothesised that there are more exposed uncovered areas on these oil droplets compared to the droplets stabilised by particles before removal of excess surfactant. The inability of the lipid particles to form a densely packed monolayer at the interface and fully cover the droplet surface could be explained by their negative charge causing electrostatic repulsions [13,51,52]. Furthermore, the lack of available surfactant molecules in the dialysed dispersions, available to provide coverage on the droplets surface or fill in the gaps between particles adsorbed at the surface (as further supported by droplet size data) could have resulted in negatively charged chains of sunflower oil protruding towards the continuous phase. Similar trends of lower ζ-potential were described for canola oil emulsion droplets stabilised by tristearin lipid particles (ranging approximately between −30 and −45 mV) compared to the particles alone when prepared with similar concentration, as the one used in this study, of the surfactants Tween® 60 (−19 mV), Brij® S20 (−3 mV) or Brij® S100 (−24 mV) [18]. On the other hand, in a study by Schröder *et al.* [14], the ζ-potential values recorded for tripalmitin particles of an

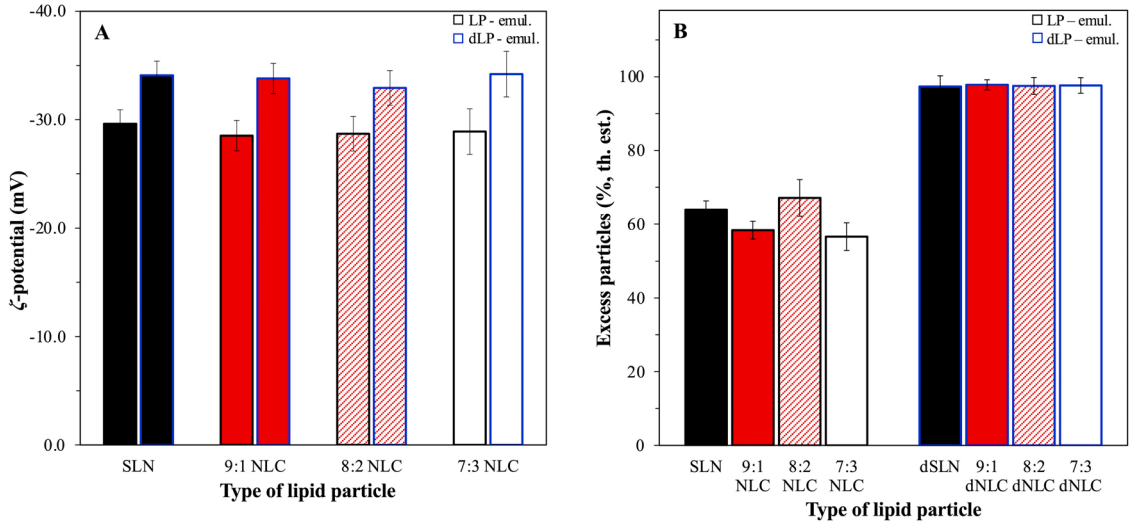

Fig. 8. (A) ζ-potential of emulsions stabilised with different types of lipid particles used as produced (LP) and after dialysis (dLP), and (B) percentage of excess particles still available in the continuous phase of the emulsions after emulsification, for different types of lipid particles used as produced before and after dialysis, based on theoretical estimations (th.est.).

average diameter of 145 nm fabricated with sodium caseinate were identical (~−36 mV) to the particle-stabilised sunflower oil emulsion droplets with average diameter of 1 μm. The difference in the reported surface charge data could be explained by the pre-treatment of sunflower oil to remove impurities, in combination with the use of a bulkier surface active species in the aforementioned study, that could have potentially resulted in more sparse surface coverage of the emulsion droplets.

The long-term storage behaviour of the particle-stabilised emulsions showed slight peak shifts for that of the unadsorbed particles and of the emulsion droplets to larger sizes over the first week (Fig. S3, Table S2). However, no further size distribution changes, and more importantly no loss of emulsion integrity with oil layer formation were recorded for up to 12 weeks (Table S2). Appearance of a thin cream layer in all formulations around the first week mark due to droplet aggregation could account for the initial size shift. As indicated above, the interfacial layer of the emulsion droplets for all systems is characterised by uncovered spots, that could be prone to coalescence [13,53,54]. Gautier *et al.* [55] described two limiting situations for when coalescence phenomena halt in silica- or latex-stabilised emulsions; either after a dense monolayer has been formed, or when emulsions flocculate due to attractive interactions or bridge formation between particles. The latter explanation could apply in the systems reported here, as on one hand particle network formation has been previously described for lipid particles fabricated with Tween® 60 [18] and on the other, droplets in close proximity can be identified in the microscopy images, confirming droplet flocculation (Fig. S3). Despite that, polarised light microscopy images at 12 weeks suggest that lipid particles still remain adsorbed at the oil-water interface, which could be due to the high ΔG_d of the particles resulting in irreversible adsorption [56].

4. Conclusions

This study explores the impact of formulation parameters, namely the lipid matrix composition and the presence of excess/remnant unadsorbed surfactant in the aqueous carrier phase, on the potential of lipid particles to act as Pickering stabilisers of o/w emulsion droplets. In regard to the effect of excess surfactant removal from the lipid particle dispersions, it was demonstrated that although some changes in the particle sizes and ζ-potential values were observed initially, possibly imposed by the dialysis process, all types of particles maintained their crystallinity and relative stability over time. The role of the lipid matrix composition, and more specifically the affinity between the lipids and the surfactant used in relation to the interfacial decoration and relative hydrophilicity of the particles was highlighted. Lipid particles containing higher liquid lipid content were shown to be more hydrophilic not only due to the introduction of the relatively more hydrophilic liquid lipid, but also owing to the entrapment of higher proportion of the available surfactant within their crystalline structure, as supported by both interfacial tension and wettability data. Despite variations in their interfacial architecture, the Pickering functionality was confirmed for both SLNs and NLCs. Lastly, although the absence of remnant surfactant from the aqueous carrier phase of the dispersions led to larger emulsion droplet sizes, the affinity of the particles for the emulsion interface was not compromised. Investigations as to how these lipid particle formulation aspects, and consequently the obtained emulsion microstructures affect the concurrent particle functionality as active carriers are the focus of the second part of this study.

CRediT authorship contribution statement

Georgia I. Sakellari: Conceptualization, Methodology, Formal analysis, Investigation, Writing – original draft. **Ioanna Zafeiri:** Writing – review & editing. **Hannah Batchelor:** Supervision, Writing – review & editing. **Fotis Spyropoulos:** Supervision, Writing – review & editing, Funding acquisition.

Declaration of Competing Interest

The authors declare that they have no known competing financial interests or personal relationships that could have appeared to influence the work reported in this paper.

Data Availability

No data was used for the research described in the article.

Acknowledgements

This work was supported by funding from the Biotechnology and Biological Sciences Research Council (BBSRC) through the Midlands Integrative Bioscience Doctoral Training Partnership (BB/M01116X/1).

Appendix A. Supporting information

Supplementary data associated with this article can be found in the online version at doi:10.1016/j.colsurfa.2022.130135.

References

[1] E. Dickinson, Food emulsions and foams: stabilization by particles, Curr. Opin. Colloid Interface Sci. 15 (2010) 40–49, https://doi.org/10.1016/j.cocis.2009.11.001.
[2] H. Jiang, Y. Sheng, T. Ngai, Pickering emulsions: versatility of colloidal particles and recent applications, Curr. Opin. Colloid Interface Sci. 49 (2020) 1–15, https://doi.org/10.1016/j.cocis.2020.04.010.
[3] G.I. Sakellari, I. Zafeiri, A. Pawlik, D. Kurukji, P. Taylor, I.T. Norton, F. Spyropoulos, Independent co-delivery of model actives with different degrees of hydrophilicity from oil-in-water and water-in-oil emulsions stabilised by solid lipid particles via a Pickering mechanism: a-proof-of-principle study, J. Colloid Interface Sci. 587 (2021) 644–649, https://doi.org/10.1016/j.jcis.2020.11.021.
[4] Y. Wei, C. Wang, X. Liu, A. Mackie, M. Zhang, L. Dai, J. Liu, L. Mao, F. Yuan, Y. Gao, Co-encapsulation of curcumin and β-carotene in Pickering emulsions stabilized by complex nanoparticles: effects of microfluidization and thermal treatment, Food Hydrocoll. 122 (2022), 107064, https://doi.org/10.1016/j.foodhyd.2021.107064.
[5] F. Spyropoulos, D. Kurukji, P. Taylor, I.T. Norton, Fabrication and utilization of bifunctional protein/polysaccharide coprecipitates for the independent codelivery of two model actives from simple oil-in-water emulsions, Langmuir 34 (2018) 3934–3948, https://doi.org/10.1021/acs.langmuir.7b04315.
[6] G.I. Sakellari, I. Zafeiri, H. Batchelor, F. Spyropoulos, Formulation design, production and characterisation of solid lipid nanoparticles (SLN) and nanostructured lipid carriers (NLC) for the encapsulation of a model hydrophobic active, Food Hydrocoll. Health (2021), 100024, https://doi.org/10.1016/j.fhfh.2021.100024.
[7] A. Borges, V. de Freitas, N. Mateus, I. Fernandes, J. Oliveira, Solid lipid nanoparticles as carriers of natural phenolic compounds, Antioxidants 9 (2020) 998, https://doi.org/10.3390/antiox9100998.
[8] P. Jaiswal, B. Gidwani, A. Vyas, Nanostructured lipid carriers and their current application in targeted drug delivery, Artif. Cells Nanomed. Biotechnol. 44 (2016) 27–40, https://doi.org/10.3109/21691401.2014.909822.
[9] J. Weiss, E.A. Decker, D.J. McClements, K. Kristbergsson, T. Helgason, T. Awad, Solid lipid nanoparticles as delivery systems for bioactive food components, Food Biophys. 3 (2008) 146–154, https://doi.org/10.1007/s11483-008-9065-8.
[10] R. Gupta, D. Rousseau, Surface-active solid lipid nanoparticles as Pickering stabilizers for oil-in-water emulsions, Food Funct. 3 (2012) 302–311, https://doi.org/10.1039/c2fo10203j.
[11] I. Zafeiri, P. Smith, I.T. Norton, F. Spyropoulos, Fabrication, characterisation and stability of oil-in-water emulsions stabilised by solid lipid particles: the role of particle characteristics and emulsion microstructure upon Pickering functionality, Food Funct. 8 (2017) 2583–2591, https://doi.org/10.1039/c7fo00559h.
[12] A. Pawlik, D. Kurukji, I. Norton, F. Spyropoulos, Food-grade Pickering emulsions stabilised with solid lipid particles, Food Funct. 7 (2016) 2712–2721, https://doi.org/10.1039/c6fo00238b.
[13] A. Schröder, J. Sprakel, K. Schroën, J.N. Spaen, C.C. Berton-Carabin, Coalescence stability of Pickering emulsions produced with lipid particles: a microfluidic study, J. Food Eng. 234 (2018) 63–72, https://doi.org/10.1016/j.jfoodeng.2018.04.007.
[14] A. Schröder, M. Laguerre, J. Sprakel, K. Schroën, C.C. Berton-Carabin, Pickering particles as interfacial reservoirs of antioxidants, J. Colloid Interface Sci. 575 (2020) 489–498, https://doi.org/10.1016/J.JCIS.2020.04.069.
[15] A. Schröder, J. Sprakel, K. Schroën, C.C. Berton-Carabin, Tailored microstructure of colloidal lipid particles for Pickering emulsions with tunable properties, Soft Matter 13 (2017) 3190–3198, https://doi.org/10.1039/c6sm02432g.
[16] D. Johansson, B. Bergenståhl, Sintering of fat crystal networks in oil during post-crystallization processes, J. Am. Oil Chem. Soc. 72 (1995) 911–920, https://doi.org/10.1007/BF02542069.

[17] G. Li, W.J. Lee, C.P. Tan, O.M. Lai, Y. Wang, C. Qiu, Tailored rigidity of W/O Pickering emulsions using diacylglycerol-based surface-active solid lipid nanoparticles, Food Funct. 12 (2021) 11732–11746, https://doi.org/10.1039/d1fo01883c.
[18] H. Lim, M. Jo, C. Ban, Y.J. Choi, Interfacial and colloidal characterization of oil-in-water emulsions stabilized by interface-tunable solid lipid nanoparticles, Food Chem. 306 (2020), 125619, https://doi.org/10.1016/j.foodchem.2019.125619.
[19] I. Zafeiri, C. Horridge, E. Tripodi, F. Spyropoulos, Emulsions co-stabilised by edible pickering particles and surfactants: the effect of HLB value, Colloid Interface Sci. Commun. 17 (2017) 5–9, https://doi.org/10.1016/j.colcom.2017.02.001.
[20] R. Pichot, F. Spyropoulos, I.T. Norton, Competitive adsorption of surfactants and hydrophilic silica particles at the oil–water interface: interfacial tension and contact angle studies, J. Colloid Interface Sci. 377 (2012) 396–405, https://doi.org/10.1016/j.jcis.2012.01.065.
[21] J. Milsmann, K. Oehlke, K. Schrader, R. Greiner, A. Steffen-Heins, Fate of edible solid lipid nanoparticles (SLN) in surfactant stabilized o/w emulsions. Part 1: interplay of SLN and oil droplets, Colloids Surf. A Physicochem Eng. Asp. 558 (2018) 615–622, https://doi.org/10.1016/j.colsurfa.2017.05.073.
[22] S.M. Dieng, N. Anton, P. Bouriat, O. Thioune, P.M. Sy, N. Massaddeq, S. Enharrar, M. Diarra, T. Vandamme, Pickering nano-emulsions stabilized by solid lipid nanoparticles as a temperature sensitive drug delivery system, Soft Matter 15 (2019) 8164–8174, https://doi.org/10.1039/c9sm01283d.
[23] B.P. Binks, T.S. Horozov, Colloidal Particles at Liquid Interfaces, Cambridge University Press, 2006, https://doi.org/10.1017/cbO9780511536670.
[24] T. Helgason, T.S. Awad, K. Kristbergsson, D.J. McClements, J. Weiss, Effect of surfactant surface coverage on formation of solid lipid nanoparticles (SLN, J. Colloid Interface Sci. 334 (2009) 75–81, https://doi.org/10.1016/j.jcis.2009.03.012.
[25] E. Dickinson, An Introduction to Food Colloids, Oxford University Press, 1992.
[26] C. Ban, S. Lim, P.S. Chang, Y.J. Choi, Enhancing the stability of lipid nanoparticle systems by sonication during the cooling step and controlling the liquid oil content, J. Agric. Food Chem. 62 (2014) 11557–11567, https://doi.org/10.1021/jf503489v.
[27] C. Ban, M. Jo, S. Lim, Y.J. Choi, Control of the gastrointestinal digestion of solid lipid nanoparticles using PEGylated emulsifiers, Food Chem. 239 (2018) 442–452, https://doi.org/10.1016/j.foodchem.2017.06.137.
[28] A.M. Nik, S. Langmaid, A.J. Wright, Nonionic surfactant and interfacial structure impact crystallinity and stability of β-carotene loaded lipid nanodispersions, J. Agric. Food Chem. 60 (2012) 4126–4135, https://doi.org/10.1021/jf204810m.
[29] K. Westesen, B. Siekmann, Investigation of the gel formation of phospholipid-stabilized solid lipid nanoparticles, Int. J. Pharm. 151 (1997) 35–45, https://doi.org/10.1016/S0378-5173(97)04890-4.
[30] H. Bunjes, F. Steiniger, W. Richter, Visualizing the structure of triglyceride nanoparticles in different crystal modifications, Langmuir 23 (2007) 4005–4011, https://doi.org/10.1021/la062904p.
[31] K. Szymczyk, A. Taraba, Aggregation behavior of Triton X-114 and Tween 80 at various temperatures and concentrations studied by density and viscosity measurements, J. Therm. Anal. Calor. 126 (2016) 315–326, https://doi.org/10.1007/S10973-016-5631-3.
[32] G. v Lowry, R.J. Hill, S. Harper, A.F. Rawle, C.O. Hendren, F. Klaessig, U. Nobbmann, P. Sayre, J. Rumble, Guidance to improve the scientific value of zeta-potential measurements in nanoEHS, Environ. Sci. Nano 3 (2016) 953–965, https://doi.org/10.1039/C6EN00136J.
[33] Q. Yuan, R.A. Williams, CO-stabilisation mechanisms of nanoparticles and surfactants in Pickering Emulsions produced by membrane emulsification, J. Memb. Sci. 497 (2016) 221–228, https://doi.org/10.1016/j.memsci.2015.09.028.
[34] P. Prombutara, Y. Kulwatthanasal, N. Supaka, I. Sramala, S. Chareonpornwattana, Production of nisin-loaded solid lipid nanoparticles for sustained antimicrobial activity, Food Control 24 (2012) 184–190, https://doi.org/10.1016/j.foodcont.2011.09.025.
[35] E.B. Souto, S.A. Wissing, C.M. Barbosa, R.H. Müller, Evaluation of the physical stability of SLN and NLC before and after incorporation into hydrogel formulations, Eur. J. Pharm. Biopharm. 58 (2004) 83–90, https://doi.org/10.1016/j.ejpb.2004.02.015.
[36] H. Salminen, T. Helgason, S. Aulbach, B. Kristinsson, K. Kristbergsson, J. Weiss, Influence of co-surfactants on crystallization and stability of solid lipid nanoparticles, J. Colloid Interface Sci. 426 (2014) 256–263, https://doi.org/10.1016/j.jcis.2014.04.009.
[37] D.J. McClements, H. Xiao, Potential biological fate of ingested nanoemulsions: Influence of particle characteristics, Food Funct., R. Soc. Chem. (2012) 202–220, https://doi.org/10.1039/c1fo10193e.
[38] I. Zafeiri, J.E. Norton, P. Smith, I.T. Norton, F. Spyropoulos, The role of surface active species in the fabrication and functionality of edible solid lipid particles, J. Colloid Interface Sci. 500 (2017) 228–240, https://doi.org/10.1016/j.jcis.2017.03.085.
[39] J. Milsmann, K. Oehlke, R. Greiner, A. Steffen-Heins, Fate of edible solid lipid nanoparticles (SLN) in surfactant stabilized o/w emulsions. Part 2: Release and partitioning behavior of lipophilic probes from SLN into different phases of o/w emulsions, Colloids Surf. A Physicochem Eng. Asp. 558 (2018) 623–631, https://doi.org/10.1016/j.colsurfa.2017.05.050.
[40] B.P. Binks, Particles as surfactants - Similarities and differences, Curr. Opin. Colloid Interface Sci. 7 (2002) 21–41, https://doi.org/10.1016/S1359-0294(02)00008-0.
[41] S.U. Pickering, CXCVI. - Emulsions, J. Chem. Soc. Trans. 91 (1907) 2001–2021, https://doi.org/10.1039/CT9079102001.
[42] B.P. Binks, J.H. Clint, Solid wettability from surface energy components: relevance to pickering emulsions, Langmuir 18 (2002) 1270–1273, https://doi.org/10.1021/la011420k.
[43] A. Shirvani, S.A.H. Goli, J. Varshosaz, L. Salvia-Trujillo, O. Martín-Belloso, Fabrication of edible solid lipid nanoparticle from beeswax/propolis wax by spontaneous emulsification: optimization, characterization and stability, Food Chem. 387 (2022), 132934, https://doi.org/10.1016/j.foodchem.2022.132934.
[44] R. Aveyard, J.H. Clint, T.S. Horozov, Aspects of the stabilisation of emulsions by solid particles: effects of line tension and monolayer curvature energy, Phys. Chem. Chem. Phys. 5 (2003) 2398–2409, https://doi.org/10.1039/b210687f.
[45] J.B. Brubach, V. Jannin, B. Mahler, C. Bourgaux, P. Lessieur, P. Roy, M. Ollivon, Structural and thermal characterization of glyceryl behenate by X-ray diffraction coupled to differential calorimetry and infrared spectroscopy, Int. J. Pharm. 336 (2007) 248–256, https://doi.org/10.1016/j.ijpharm.2006.11.057.
[46] J. Tan, M. Zhang, J. Wang, J. Xu, D. Sun, Temperature induced formation of particle coated non-spherical droplets, J. Colloid Interface Sci. 359 (2011) 171–178, https://doi.org/10.1016/j.jcis.2011.03.065.
[47] P.Y. Liu, R.Y. Yang, A.B. Yu, Self-diffusion of wet particles in rotating drums, Phys. Fluids 25 (2013), 063301, https://doi.org/10.1063/1.4807596.
[48] I.T. Norton, F. Spyropoulos, P.W. Cox, Effect of emulsifiers and fat crystals on shear induced droplet break-up, coalescence and phase inversion, Food Hydrocoll. 23 (2009) 1521–1526, https://doi.org/10.1016/j.foodhyd.2008.09.014.
[49] X. Li, H. Li, Q. Xiao, L. Wang, M. Wang, X. Lu, P. York, S. Shi, J. Zhang, Two-way effects of surfactants on Pickering emulsions stabilized by the self-assembled microcrystals of a-cyclodextrin and oil, Phys. Chem. Chem. Phys. 16 (2014) 14059, https://doi.org/10.1039/c4cp00807c.
[50] A.T. Florence, J.A. Rogers, Emulsion stabilization by non-ionic surfactants: experiment and theory, J. Pharm. Pharmacol. 23 (1971) 153–169, https://doi.org/10.1111/j.2042-7158.1971.tb08637.x.
[51] O.S. Deshmukh, D. van den Ende, M.C. Stuart, F. Mugele, M.H.G. Duits, Hard and soft colloids at fluid interfaces: adsorption, interactions, assembly & rheology, Adv. Colloid Interface Sci. 222 (2015) 215–227, https://doi.org/10.1016/j.cis.2014.09.003.
[52] M. Destribats, S. Gineste, E. Laurichesse, H. Tanner, F. Leal-Calderon, V. Héroguez, V. Schmitt, Pickering emulsions: what are the main parameters determining the emulsion type and interfacial properties? Langmuir 30 (2014) 9313–9326, https://doi.org/10.1021/la501299u.
[53] T.S. Horozov, B.P. Binks, Particle-Stabilized emulsions: a bilayer or a bridging monolayer? Angew. Chem. Int. Ed. 45 (2006) 773–776, https://doi.org/10.1002/anie.200503131.
[54] S.P. Nagarkar, S.S. Velankar, Morphology and rheology of ternary fluid–fluid–solid systems, Soft Matter 8 (2012) 8464–8477, https://doi.org/10.1039/c2sm25758k.
[55] F. Gautier, M. Destribats, R. Perrier-Cornet, J.F. Dechézelles, J. Giermanska, V. Héroguez, S. Ravaine, F. Leal-Calderon, V. Schmitt, Pickering emulsions with stimulable particles: from highly- to weakly-covered interfaces, Phys. Chem. Chem. Phys. 9 (2007) 6455–6462, https://doi.org/10.1039/b710226g.
[56] R. Aveyard, B.P. Binks, J.H. Clint, Emulsions stabilised solely by colloidal particles, Adv. Colloid Interface Sci. 100 (2003) 503–546, https://doi.org/10.1016/S0001-8686(02)00069-6.